

**This item is the archived peer-reviewed author-version of:**

Application of Atomic Force (AFM), Environmental Scanning Electron (ESEM) and Confocal Laser Scanning Microscopy (CLSM) in bitumen : a review of the ageing effect

**Reference:**

Pipintakos Georgios, Hasheminejad Navid, Lommaert Caitlin, Bocharova Anastassiya, Blom Johan.- Application of Atomic Force (AFM), Environmental Scanning Electron (ESEM) and Confocal Laser Scanning Microscopy (CLSM) in bitumen : a review of the ageing effect  
Micron - ISSN 0968-4328 - 147(2021), 103083  
Full text (Publisher's DOI): <https://doi.org/10.1016/J.MICRON.2021.103083>  
To cite this reference: <https://hdl.handle.net/10067/1780330151162165141>

# Application of Atomic Force (AFM), Environmental Scanning Electron (ESEM) and Confocal Laser Scanning Microscopy (CLSM) in bitumen: A review of the ageing effect

Georgios Pipintakos <sup>a</sup>, Navid Hasheminejad <sup>a,\*</sup>, Caitlin Lommaert <sup>a</sup>, Anastassiya Bocharova <sup>a</sup> and Johan Blom <sup>a</sup>

<sup>a</sup> *University of Antwerp, EMIB research group, Groenenborgerlaan 171, Antwerp 2020, Belgium*

## 1 **Abstract**

2 Undoubtedly bitumen's viscoelastic performance has received much attention in the literature. Especially, the  
3 oxidative ageing phenomenon of bitumen has been studied by several scholars from different physicochemical and  
4 mechanical perspectives due to its direct impact on asphalt performance. The microstructural patterns observed  
5 with ageing utilising different microscopic techniques have not remained unexplored, and an increasing interest  
6 has been expressed to understand the bitumen's architecture by coupling it with different theories. This review aims  
7 to provide a useful guide for the road engineer by collecting all the existing microstructural trends that have been  
8 reported upon ageing by utilising some of the most promising microscopic techniques. The study demonstrates the  
9 changes being observed for the size of the so-called bee structures via Atomic Force Microscopy (AFM). The  
10 apparent fibril microstructure captured with Environmental Scanning Electron Microscopy (ESEM) consistently  
11 reported in the literature to become denser and coarser with ageing. The existing findings of Confocal Laser  
12 Scanning Microscopy (CLSM) revealed the conflicting observations that exist for the fluorescent centres of  
13 bitumen upon oxidation, concerning their size and number. Finally, this paper provides a comparative analysis of  
14 the three techniques for bitumen applications and recommends a systematic sample preparation protocol to move  
15 towards more consistent observations between the different research groups.

16 **Keywords:** ageing, bitumen, AFM, ESEM, CLSM

## 17 **1. Introduction**

18 Bitumen is a material derived from crude oil and acts predominantly as the binding medium in asphalt pavements  
19 due to its superior viscoelastic and water-proofing performance [1]. At the same time, bitumen exists as a natural  
20 deposit, with apparent differences existing in terms of composition between refined and naturally occurring  
21 bitumens [2]. Generally, bitumen consists of about 85% carbon, 10% hydrogen, heteroatoms in lesser amounts  
22 such as nitrogen (0-2%), oxygen (0-2%), sulfur (0-9%), and traces of metals such as vanadium, iron and  
23 nickel [3,4].

24 Bitumen undergoes alterations not only in the physicochemical [5–11] and mechanical properties [12–14] but  
25 also in microstructural patterns due to the effect of different processes occurring during its production and service  
26 life. Among other existing processes (physical hardening, volatilisation, condensation), the diffusion-reaction of  
27 oxygen with bitumen, known as oxidative ageing, is an irreversible phenomenon that has been studied thoroughly  
28 over the past years. A common practice to mimic and accelerate ageing of bitumen in the lab is to use standardised  
29 procedures to capture the oxidation taking place in the initial production, mixing, transportation and paving phase  
30 and during service life due to the environmental conditions. Usually, the rolling thin-film oven test (RTFOT) [15]  
31 is used to simulate the first phase known as short-term ageing and the pressurised ageing vessel (PAV) [16] to  
32 mimic the effect of ageing after paving in situ (long-term ageing). Doubts remain whether these simulations  
33 realistically anticipate the environmental conditions in situ due to the high temperature and increased pressure that  
34 are used [17].

35 Hitherto, a number of studies suggested that chemistry and microstructure are the key-elements to unwrap the  
36 association of ageing with the bitumen's performance [18–23]. Understanding of the fundamentals is considered  
37 crucial since ageing of bitumen is one of the major causes of distress types of asphalt in situ, such as ravelling and  
38 cracking [12,21,24,25]. Coupling of the possible interactions of polar compounds produced with ageing [6,8,26–  
39 29] and the microstructural changes, may assist in understanding their role in bitumen's performance. A rather  
40 simplistic but pragmatic approach is to characterise bitumen's structure based on solubility classes by utilising  
41 different solvents. This technique was introduced already in the 70s [30] and is known nowadays as the SARA  
42 fractionation due to the four main derived solubility-based categories namely Saturates, Aromatics, Resins and  
43 Asphaltenes. Different techniques have been proposed for this classification, which can also result in slight

44 differences even for the same bituminous samples [31,32]. Many studies have highlighted that due to ageing  
45 bitumen exhibits a shift of these fractions from aromatics to resins and finally to asphaltenes, whereas saturates are  
46 considered in general unreactive and thus relatively constant employing their percentage value [20,33–36].  
47 Moreover, asphaltenes are the largest and most aromatic constituents which account primarily for the overall  
48 bitumen's viscous behaviour [37,38], and correlations of asphaltene content with viscosity have been reported [18].  
49 Resins are believed to contribute as a stabilising medium in bitumen, by means of asphaltenes micelles surrounded  
50 by them [37,39]. Controversy still exists in the bitumen community with regard to this colloidal model as  
51 researchers worldwide have questioned the validity of this theory counter-proposing different ones [40,41].

52 In parallel, microscopic applications have been considerably improved to such an extent able to gain deeper  
53 insights into the bitumen microstructure, not only in the surface but even in the bulk of bitumen upon ageing.  
54 However, obstacles still exist to understand completely what is captured on a microscale level which accounts for  
55 the bitumen's microstructure or morphology and its association with crystallising substances. For example, the lack  
56 of universal sample preparation, non-reporting of the sample's substrate nature, exact thermal history, storage time,  
57 and thickness as well as essential compositional characteristics such as the presence of crystallisable components  
58 have hampered the direct comparison of a variety of outputs published by different research groups. Difficulties in  
59 the comparison of different studies can also be generated as a result of long heating times and high temperatures  
60 during sample preparation, which can induce additional ageing. Other factors such as remaining water drops after  
61 samples' freezing, dissolved samples, insufficiently flat surfaces of the bituminous films and destruction of the  
62 sample due to the use of a highly energetic electron beam can introduce additional artefacts.

63

## 64 **2. Objectives and outline**

65 Since it became obvious during the last decades how microscopic techniques can assist in understanding the  
66 microstructural patterns in bitumen, the need to highlight the most important techniques and accompanying changes  
67 in microstructure upon ageing is of utmost importance. One able to dive into the microstructure of bitumen choosing  
68 the correct tool can afterwards consult towards a systematic modification (addition of polymers, rejuvenators,  
69 nanoparticles or other agents [42]). Furthermore, as bitumen is a non-renewable organic material, a disciplined

70 usage is required against its depletion which is stimulated additionally due to ageing. It is believed that by providing  
71 this overview, potential policy-makers will be able to make the correct decisions, knowing the material by its basics.

72 Hence, this review paper provides the framework of the three most promising microscopic applications to  
73 investigate surface microstructural traits upon ageing in bitumen. To that end, the working principles of the atomic  
74 force microscopy (AFM), environmental scanning electron microscopy (ESEM) and confocal laser scanning  
75 microscopy (CLSM) are presented herein so that the potential reader, especially the pavement engineer, can become  
76 familiar, as there is an increasing demand for them. The paper aims to gather all the reported ageing-related  
77 microstructural observations reported until now for these three techniques. It provides a comparison between them  
78 and makes recommendations for sample preparation instructions.

79 The review is outlined in the following way: first, the theoretical background of the existing microstructural  
80 theories is briefly revisited in subsection 3.1. The reader then is invited in subsection 3.2. to strengthen the  
81 knowledge concerning the wax presence in bitumen, which is believed to have an association with the microscopic  
82 observations. Section 4 is divided per microscopic technique for which the general working principles to perform  
83 a measurement are provided, followed by the reported bitumen-related applications. The remainder of each  
84 subsection is devoted to the ageing-induced microstructural changes that have been observed utilising the different  
85 microscopies. Next, section 5 provides an overview of the limitations and advantages of each microscopy when it  
86 comes to identifying ageing-related microstructural changes and attempts to propose a comprehensive protocol to  
87 increase reproducibility and repeatability between different research groups. The remainder of the paper (Section  
88 6) provides the main conclusions and recommendations that can be drawn from this review for capturing the ageing  
89 effect in bitumen's microstructure.

### 90 **3. Theoretical background**

91 To gain a better understanding of the main findings by the use of microscopies in bitumen and the effort to link  
92 them with possible microstructural models the governing theories and the effect of wax regarding these  
93 observations are briefly reviewed.

### 94 **3.1. Microstructural theories**

95        Already in the dawn of the 20<sup>th</sup> century, a colloidal structure for bitumen was proposed [43], with more detailed  
96 descriptions of this assumption documented by Nellensteyn a decade later [44]. The latter study supported that  
97 asphaltenes constitute a colloidal suspension together with the maltenes, which consists of aromatics, resins and  
98 saturates, while resins play a stabilising role in bitumen [45]. This idea was developed further based on the  
99 association with the rheological response which was believed to vary between sol bitumens (Newtonian behavior)  
100 and non-linear gel ones (non-Newtonian behavior), while most of the bitumens behaved in a situation between the  
101 two cases, known as sol-gel [46,47]. The difference between the two extrema was attributed to the interconnectivity  
102 of the asphaltenes micelles in the gel phase, whereas the full dispersion and successively lack of interaction of the  
103 asphaltenes micelles was responsible for a sol type of bitumen's structure. The intermediate situation implied the  
104 co-existence of the two [46]. Relationships between the different colloid types in bitumen and the ratio of  
105 asphaltenes and saturates content over the sum of resins and aromatics were established, to characterise bitumen's  
106 colloidal stability [48]. It is widely accepted nowadays that the gel character is apparent for ratios greater than 1.2  
107 and the sol one for values smaller than 0.7 [48,49].

108        The main opponents of the colloidal model argued already in the 90s that bitumen is a purely homogeneous  
109 fluid known as dispersed polar fluid, which gave its name in this theory concerning the intrinsic architecture of  
110 bitumen [40,41,50]. The main argumentation in disregarding the colloidal theory was generated around the lack  
111 of an elastic plateau for the gel bitumens [37] and the lack of a thermodynamic basis of separation of bitumen in  
112 different phases. More specifically, a hypothesised phase separation would reduce the system's entropy and would  
113 require an enthalpy compensation which is contrary to the micelle theory where asphaltenes are considered to be  
114 gathered. In the homogeneous fluid theory, the bitumen molecules are considered to be in a mutual solution  
115 including a range of solubility parameters in such a way that everything is kept soluble. Additionally, they believed  
116 that the monotonic time dependence and the unimodal relaxation spectrum with regard to the viscoelastic response  
117 of bitumen were the basis to support such a homogeneous theory.

118        The most recent colloid theories, known as the Yen-Mullins model, support that asphaltenes play a dominant  
119 role as 'island' structures in the molecular architecture of crude oils and therefore also of bitumen [51,52].  
120 Asphaltenes are believed to appear in 'islands' which in sufficient concentration can form nanoaggregates and in

121 higher concentration clusters [52,53]. Moreover, the role of resins as stabilising medium of asphaltene  
122 nanoaggregates is no longer acceptable. Validation of disk-shaped core-shell structures for the asphaltene  
123 nanoaggregates has also been provided experimentally with advanced techniques of Small-Angle Neutron and X-  
124 Ray Scattering [54] as well as with Nuclear Magnetic Resonance studies [55].

### 125 **3.2. Waxes in bitumen**

126 Bitumen, apart from the reported solubility-based SARA fractions, can include another specific fraction which  
127 is called wax. Petroleum wax can appear in the type of paraffinic or microcrystalline wax [56–58]. The former  
128 refers to the linear n-alkanes with a few or no branches, whereas the latter to the aliphatic hydrocarbons with a  
129 significant amount of iso- and cycloparaffins [4]. The paraffinic wax is usually crystallised in flat plates and is  
130 known as macrocrystalline wax. Microcrystalline wax, on the other hand, crystallises in small needles.

131 Microscopic studies have also revealed different geometries for the formed crystals of apparent size 1-10  $\mu\text{m}$   
132 [59,60]. Among the factors that affect the crystallisation of the wax in bitumen, as well as the shape and size of  
133 crystals, are the thermal history, cooling conditions and rate, as well as the storage time of the samples.

134 In practice, the Differential Scanning Calorimetry (DSC) is used as an effective tool to detect the wax content  
135 in bitumen based on the occurrence of melting signals and derived melting enthalpies [61]. From various DSC  
136 studies, it has been measured that paraffinic waxes in waxy bitumens account for about 5% wt or less and their  
137 effect on rheology has been identified mainly to the low-temperature physical hardening [62]. In some bituminous  
138 binders, the effect of waxes on rheology has also been seen as a loss in time-temperature superposition in the  
139 melting range of the wax [63].

140 Wax has also been reported to display interrelationships with microscopic findings on the bitumen surface. A  
141 previous study supported the hypothesis that crystalline structure will move towards the surface in order to reach  
142 an equilibrium with the wax molecules still in solution in the bitumen matrix [26]. In parallel, it was believed that  
143 ageing creates a thin film of less soluble hydrocarbon molecules at the surface of a bitumen film, preventing the  
144 microstructures from floating to the surface.

## 145 **4. Microscopic techniques**

### 146 **4.1. AFM**

#### 147 **4.1.1. Working principles**

148 Imaging with the AFM microscope has evolved over the past years but the general working principles remain  
149 the same, rooted back in its invention in 1986 [64]. More specifically, the imaging of the target uses a cantilever,  
150 with a sharp tip (colloidal probe) that is used to scan the sample surface by interacting with it. When the cantilever  
151 experiences a force between the tip and the sample, measured by a laser beam that is placed at the end of the  
152 cantilever, it deflects and shifts up according to the Hooke's law. This results in a deviation of the laser beam from  
153 its original position, which is measured as a voltage. This voltage is translated into a variety of forces (e.g.  
154 mechanical contact force, capillary forces etc.) or relative height and an image can be made based on all the  
155 measured differences [64,65].

156 There are different operational modes of an AFM, but among others (near-contact, pulsed force, lateral force  
157 mode) the most common ones are discussed here, namely the dynamic (tapping) and the static (contact) mode [22].  
158 With contact mode, one refers to the mode where the tip stays in contact with the sample at constant load, while  
159 the surface is moving in the plane directions. This mode is able to generate both frictional and topographic data.  
160 Tapping mode, on the other hand, occurs when the cantilever, oscillating up and down at its resonance frequency,  
161 is gently tapped on the surface to reach contact and then in the plane directions when the tip is lifted away from  
162 contact. This mode provides phase and topographic data and generally reduces the chance to destroy the surface  
163 compared to the static mode where the developing forces are higher [65].

#### 164 **4.1.2. Bitumen application**

165 The microstructure of bitumen is still a subject that is not fully understood and completed. Over the years, there  
166 were a lot of attempts to examine the microstructure of bitumen, with the most commonly used technique being  
167 the optical microscope. AFM proved to be a promising alternative and was adopted by bitumen researchers soon  
168 after its invention [66]. The results give information about the topography and phase contrast of the sample and are  
169 therefore especially useful for multi-phase materials such as bitumen. Using AFM, experts aimed to characterize  
170 the topography, stiffness, tackiness and molecular interaction at the micro-level of bitumen [67]. In parallel,

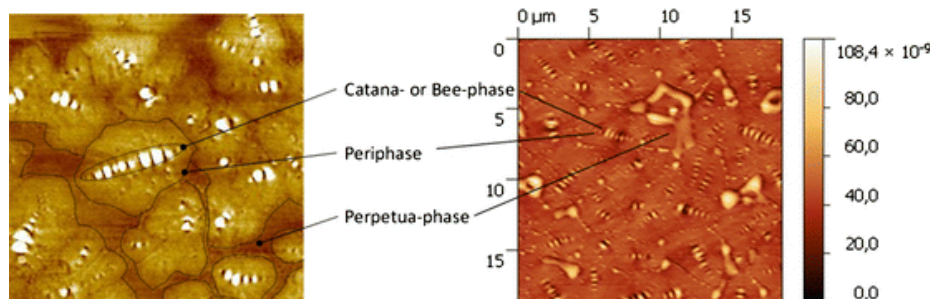


171 mechanical properties of bitumen such as adhesion, rigidity, hardness and modulus of elasticity can be estimated  
172 employing AFM with the nanoindentation technique [68]. This technique penetrates the bitumen surface with a tip  
173 of defined geometry [69].

174 The fact that AFM is time-efficient and experiments can be performed at different temperatures, even at room  
175 temperature, makes its use favorable. However, it was proven that the handling temperature has a significant impact  
176 on the final results, and as such for a fair comparison between AFM findings by different research groups, the  
177 thermal history, among other factors, during the sample preparation must remain the same. Some limitations of  
178 AFM bitumen application are that it delivers surface images, possibly not depicting the microstructure in the bulk  
179 of bitumen [70] and that the surface of the prepared sample should be relatively smooth and of sufficient thickness  
180 to exclude surface-driven effects [71,72]. Moreover, tacky and liquid samples cannot be measured with an AFM in  
181 the tapping mode.

182 Another appealing reason for the AFM application in bitumen is the relatively simple sample preparation.  
183 Attention should be though given in the consistency of the preparation procedures as it may introduce differences  
184 if the handling procedure and storage conditions vary significantly between the samples. In general, sample  
185 preparation can be done by two different techniques for bituminous binders, either the spin or the heat casting  
186 method. Spin casting includes a spinning plate, where the sample is cast on. The centrifugal forces of the plate  
187 provoke the sample to spread evenly so that it eventually results in a thin film for the imaging. Beforehand, the  
188 bitumen is dissolved in a solvent which evaporates after the spinning. Allen and his coworkers suggested the  
189 elimination of the residual solvent to preserve the sample in an airtight heated vacuum desiccator with a purification  
190 step with dry nitrogen after [73].

191 For the heat casting method, the bitumen is heated and stirred at a temperature  $T=110-130\text{ }^{\circ}\text{C}$ , according to the  
192 bitumen type to be workable, and profoundly mixed so that a specimen has no more oxidants or dust compared to  
193 a replica of the same bitumen tank [74]. Next, a bitumen drop of 15-30 mg is placed on a conductive sample holder  
194 and held horizontally on a heating plate (set at the same temperature with the heating  $T$  of bitumen) so it would  
195 spread evenly and become a flat surface. The samples are normally tested directly in the AFM and then held in a  
196 dust-free environment before testing again at different time intervals so that the microstructures can settle and their  
197 evolution can appear on the bitumen's surface.



198 Figure 1: Typical phases of surface bitumen microstructure before [left] and after ageing [right] in phase contrast and topography respectively  
 199 [74].

200 Concerning the observed AFM microstructure in bitumen is generally accepted that rippled, wavy-like  
 201 structures exist on the bitumen surface, widely known as ‘bees’ due to the yellow and black color with which they  
 202 were first represented by Loeber and his colleagues [66]. Typically, 3 to 4 phases can be identified with AFM  
 203 imaging: the catanaphase (bee-structure), the periphase (around catanaphase), and the perpetua phase which can be  
 204 distinguished in the paraphase (solvent regions) and the salphase (high phase contrast spots) [74,75]. A simplified  
 205 example of this phase detection is given in the example Figure 1 before and after ageing. Whether the bee-shape  
 206 structures have an association with the bitumen fractions was a matter of debate for many years, with lots of studies  
 207 to believe that asphaltenes are responsible for the bees as they appear as a result of this fraction [76,77]. The  
 208 opponents of this claimed that the paraffinic wax crystals present in bitumen are the reason behind the bee-  
 209 structures by providing support via DSC measurements and the addition of waxes to a wax-free bitumen [74,78,79],  
 210 while other scholars also supported this theory with the wrinkling of the surface [80–82]. The wax crystallisation  
 211 seems to gain support from the most recent studies as the main reason behind the bee structure formation [83,84].

#### 212 4.1.3. Ageing-induced microstructure

213 Since the main goal of this review is to use the microscopes as a tool to trace ageing-related microstructures, a  
 214 summary of past AFM works reporting mainly the consequence of ageing on the bee-structure as well as on other  
 215 air-cooled surface-related properties, such as phase stiffness, are presented in Table 1.

216 It becomes obvious from most of the past works that ageing affects the bee-like structures, whereas limited  
 217 studies supported that ageing has no effect on the bee microstructure [85]. Yet controversy exists whether prolonged

218 and more severe ageing increases [68,86–90], decreases [91,92] or fluctuates [73,93,94] the length and area of the  
 219 bee-structures. Part of the studies having investigated ageing-related AFM microstructures argue that the bee  
 220 structures are attributed to asphaltenes [87,89,93,95] while others associated them with the waxy molecules that  
 221 bitumen may contain [26,86,92,93], which is also the governing theory nowadays. It is worth mentioning here that  
 222 relationships of the microstructural changes with the SARA fractions have also been reported as a result of ageing  
 223 [85,93,96]. Moreover, a number of studies [68,73,85,89–91,95–97] found changes with ageing in the surface  
 224 roughness and stiffness, adhesive and cohesive strength and force, with most of them claiming an increase of these  
 225 properties, while the rigidity of bitumen was related to the bitumen morphology and its components.

226

227

228 Table 1: Summary of previous works with regard to AFM bitumen observations with ageing.

Research work	Bitumen information	Ageing treatment	AFM mode	Testing temperature	Key conclusions
[93]	A virgin binder 60/80, aged and rejuvenated with different rejuvenator percentages	Thin-film oven test (TFOT) at 163°C for 3, 12 and 15 hours	Tapping mode	Room temperature	<ul style="list-style-type: none"> <li>▪ The bee phase is coated by a thick layer which is getting thinner with ageing and this is related to the changes of maltenes</li> <li>▪ Bee structures are attributed both to asphaltenes and wax crystallisation</li> <li>▪ The microstructure varies at diverse ageing stages</li> <li>▪ Rejuvenation does not affect the microstructure (size, quantity of bee-structures) compared to the aged samples</li> </ul>
[86]	Two styrene-butadiene-styrene (SBS) commercial bitumens from different plants of penetration grade around 50, modified with waste engine oil (WEO)	Standard RTFOT, PAV and 2 x PAV	Tapping mode	Not specified, prior cooling with nitrogen gas was used for 6 hours	<ul style="list-style-type: none"> <li>▪ The bee structure proportion and length increased with ageing as a possible result of volatilisation and polymerisation</li> <li>▪ WEO alters the microstructure of bitumen vanishing the bee-structure.</li> </ul>
[91]	Three bitumens with penetration grade of 50, 70 and 90	Self-developed ageing equipment including UV at 65 °C at different time intervals up to 720 hours	Peak force mode	Room temperature	<ul style="list-style-type: none"> <li>▪ Two parts were identified in aged samples: the valley areas and the aged film areas</li> <li>▪ Ageing reduced the surface roughness of the valley areas of the bitumen</li> <li>▪ Ageing decreases the area and length of the bee-structure appeared in bitumen with penetration around 50</li> <li>▪ The maximum adhesion force in the valley areas was 2-3 times greater than in aged film areas</li> </ul>

					<ul style="list-style-type: none"> <li>Hardness in the aged film area was 2-4 times greater and modulus measured by AFM was 1-2 times greater than in the valley areas</li> </ul>
[87]	One base bitumen with penetration grade around 65 and its SBS modified bitumens with penetration grade around 60 and 55	RTFOT, PAV at 60 °C at different time intervals up to 2000 hours	Static mode	Room temperature	<ul style="list-style-type: none"> <li>The unmodified bitumen appeared bigger tubers with ageing compared to the aged SBS-modified bitumen in 3D AFM images</li> <li>The size of the bee-structure was increased with ageing for the conventional bitumen and appeared for the SBS only after PAV.</li> <li>The bee-structures were attributed to asphaltene micelles</li> </ul>
[88]	One conventional bitumen with penetration grade around 90	TFOT at 163°C up to 20 hours	Tapping mode	Room temperature	<ul style="list-style-type: none"> <li>The height of the bee-structure is fluctuating with ageing whereas the areas away from the 'bees' keep relatively stable height with ageing</li> <li>The bee-structure aggregate and become bigger with ageing (area)</li> <li>The roughness and maximum amplitude gradually increase with ageing</li> <li>There is an negative relationship with the increase of microstructural and technical indexes i.e. increasing area of bee-structure with decreasing penetration</li> </ul>
[97]	Three bitumens: one commercial of penetration grade 60/70, one recovered after 7 years in situ with original penetration 60/70 and a recovered after 36 years with original penetration 80/100	For the non-recovered: standard RTFOT and PAV	Tapping and contact mode	Controlled environment (24°C, 71% humidity)	<ul style="list-style-type: none"> <li>Ageing increases the adhesive and cohesive strength of the samples</li> <li>Ageing increases the spatial variations of the nanoscale sample properties i.e. the plasticity index during the indentation process</li> </ul>
[96]	Two bitumens with penetration grade of 63 and 87	Standard RTFOT and PAV, UV aged at 80 °C after TFOT	Tapping mode	Room temperature	<ul style="list-style-type: none"> <li>The overall surface stiffness increased with ageing</li> <li>PAV ageing effect was bitumen-dependent with regard to the single phase trend in contrast to TFOT which contributed clearly to a single-phase trend for both bitumens</li> <li>UV radiation resulted in a contrasted matrix and dispersed phase (phase separation)</li> <li>Relationships between microstructural changes and SARA compositions were found</li> </ul>
[92]	One unmodified and one modified with organo-montmorillonite (OMMT) bitumen of penetration grade 63	TFOT followed by UV aged at 80 °C	Tapping mode	Room temperature	<ul style="list-style-type: none"> <li>Correlations were found between the waxy molecules of the separated asphaltene fraction and the bee-structure of the unmodified bitumen</li> </ul>

					<ul style="list-style-type: none"> <li>▪ The dimension and amount of bee-structures were reduced upon ageing as the result of crystallisation of waxes</li> <li>▪ The contrast between the matrix and dispersed phase was reduced with ageing</li> <li>▪ These changes were prevented in the OMMT-modified bitumen, demonstrating a bitumen ageing enhancement</li> </ul>
[26]	A wax-including 70/100 bitumen (5,4% wax)	UV aged, unaged samples conditioned in argon environment for 15 and 30 days at 20°C	Tapping mode	Room temperature	<ul style="list-style-type: none"> <li>▪ Water soluble thin films are formed with ageing</li> <li>▪ Ageing creates a thin surface film acting as a barrier for the microstructures to freely float on it, thus under UV and oxygen the wax-induced microstructures decrease until they disappeared</li> <li>▪ Through washing of the aged surface, microstructures reappeared</li> </ul>
[89]	Conventional bitumen 50/70	Standard RTFOT and PAV	Tapping and contact mode	Room temperature	<ul style="list-style-type: none"> <li>▪ Ageing increases the average size of the asphaltene micelles which are in sol state in the unaged sample</li> <li>▪ After PAV these micelles become interconnected in a network with open voids covered by the hydrocarbon matrix</li> <li>▪ The hydrocarbon matrix has higher loss modulus than the asphaltene micelles without ageing while the opposite trend holds upon ageing</li> <li>▪ The friction coefficient reduced in half after RTFOT and remained unchanged with PAV</li> <li>▪ Ageing increased the stiffness of the bitumen film and its apparent viscosity</li> </ul>
[85]	Conventional bitumen PG64-22 and field aged for 6 months after RTFOT	Standard RTFOT and PAV	Contact mode	Room temperature	<ul style="list-style-type: none"> <li>▪ AFM-derived adhesion and stiffness increased with ageing</li> <li>▪ Bee-structures were not considered to appear due to ageing</li> <li>▪ Bee-structures were correlated with the aromatic fraction</li> <li>▪ Adhesion and rigidity were related with the bitumen components</li> <li>▪ The catana-phase is associated with the stiffness and adhesion</li> </ul>
[68]	Two conventional bitumens PG64	Standard RTFOT and PAV	Contact and pulsed force mode	Room temperature	<ul style="list-style-type: none"> <li>▪ Adhesion and stiffness increased with ageing</li> <li>▪ Ageing increased the length of catana-phase</li> <li>▪ AFM modulus of elasticity was increasing with ageing</li> </ul>
[95]	Four conventional bitumens with penetration grades 30, 50, 70 and 90	Standard RTFOT and PAV	Tapping mode	Room temperature	<ul style="list-style-type: none"> <li>▪ AFM-derived cohesion and adhesion force increased with RTFOT ageing</li> </ul>

					<ul style="list-style-type: none"> <li>▪ The adhesion force decreases with PAV whereas the cohesion keeps increasing with PAV as a result of the asphaltene association</li> <li>▪ The ageing-induced reduction in adhesion force was found in the catana, peri and para phase</li> </ul>
[73]	Three SHRP bitumens of different performance and crude oil [3]	Standard RTFOT and PAV	Force measurement mode	Room temperature	<ul style="list-style-type: none"> <li>▪ Prior to ageing two phases are detected a continuous and a dispersed one</li> <li>▪ Long-term ageing introduces microstructural changes (phase dispersion, phase clustering and materialisation) which are bitumen-dependent</li> <li>▪ A third phase in long term ageing can be observed; the bee-structure</li> <li>▪ Ageing increases the stiffness of both the continuous and dispersed phase</li> </ul>
[94]	One virgin bitumen, one blended virgin - extracted from reclaimed asphalt bitumen (50/50), one extracted bitumen from reclaimed asphalt pavement (RAP) and two extracted from laboratory aged mixtures	Extracted after ageing the mixture with short-term oven ageing (4 hours at 135°C) and long-term oven ageing (5 days at 85°C) [98]	Tapping mode	Room temperature	<ul style="list-style-type: none"> <li>▪ The extracted recycled and aged binders showed no bee-structures compared to the virgin and RAP binders</li> <li>▪ The bee-structures were different in height and size</li> </ul>
[90]	One SBS-modified bitumen with penetration grade 54	Standard RTFOT and PAV	Tapping mode	Room temperature	<ul style="list-style-type: none"> <li>▪ The overall roughness increased with ageing possibly as a result of polymer degradation</li> <li>▪ Longer structures occur with ageing</li> <li>▪ PAV ageing increases the number of microstructures</li> </ul>

## 229 4.2. ESEM

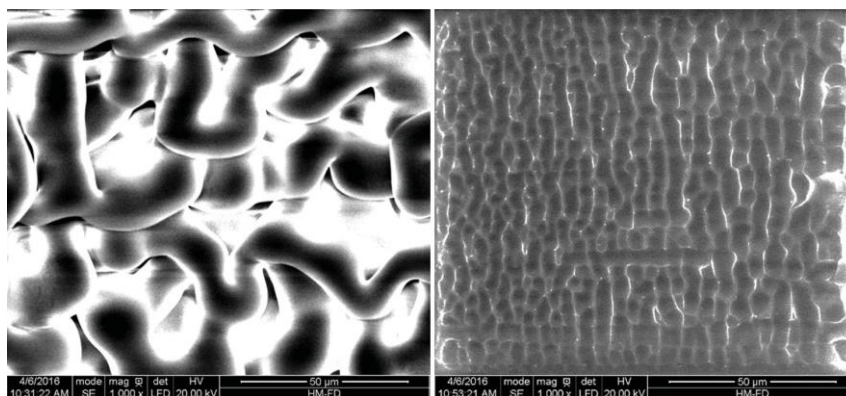
### 230 4.2.1. Working principles

231 Another promising microscopic technique, invented in the mid-80s, is the environmental scanning electron  
232 microscopy (ESEM) [99]. The advantage of this microscopy versus traditional scanning electron microscopy  
233 (SEM) is the choice of sample environment by means of temperature, pressure and gas flow, while simultaneously  
234 the necessity of high vacuum conditions is overcome [100]. It is even possible to investigate samples containing  
235 volatile components without using any additional conductive coating. Additionally, the examined sample can be  
236 tested in different states (wet, oily) and environments with gas flow and pressure up to 50 torr and temperature up  
237 to 1500 °C [101,102].

238 The working principles and manufacturing are based on the classic SEM, however, the target pressures in the  
239 electron beam tube are ensured in ESEM by isolation valves and differential pumping. Moreover, in ESEM multiple  
240 Pressure Limiting Apertures are used and the sample chamber is separated from the column which is maintained  
241 in high vacuum to preserve the electron beam from scattering [103]. A gaseous environment is used around the  
242 sample, whereas the electron gun is maintained at standard pressures around  $10^{-6}$  torr [102]. An environmental  
243 secondary detector (ESD) is used to monitor the variety of signals resulting from the beam-sample interaction  
244 which has the capability of performing also in a non-vacuum environment. The ESD collects the emitted secondary  
245 electron signal which is gathered to an electron amplifier. Finally, the output signal can be constructed to a virtual  
246 image of the sample surface.

#### 247 4.2.2. Bitumen application

248 Soon it became obvious that the advantages of ESEM in bitumen samples were numerous compared to SEM, as  
249 the sample could be tested in its natural state without de-oiling or conductive coating. As such, the benefits of the  
250 handy sample preparation allow a greater number of possibilities to be captured with ESEM under sample freezing,  
251 heating and other effects [104]. ESEM allows the microstructural analysis of the fracture, the distribution of  
252 possible containing particles, the determination of the adhesive properties, of the healing effect and others [103].  
253 The most apparent ESEM bituminous microstructures, as a result of the subsection to the electron beam, look like  
254 fibrils. The density, size and shape, as well as the required time for the fibrils to appear and stabilise, have been  
255 studied with ESEM greatly the last decade [105,106]. An example of the fibril microstructure in ESEM is illustrated  
256 in Figure 2.



257 Figure 2: ESEM fibril microstructure of an unaged bitumen [left] and upon oxidation [right] [104].

258  
259       Rozeveld and his coworkers found that the alignment of the fibrils with the direction of tensile stresses subjected  
260 to a bitumen sample is clearly due to the bitumen microstructure and not the electron beam [107]. This was  
261 understood as the volatilisation of the lighter molecules by localised heating of the sample by the electron beam.  
262 Based on this hypothesis, the apparent ESEM bitumen fibrils were initially interpreted by the scientific community  
263 to have an association with asphaltenes [107], the heaviest bitumen SARA fraction, while later it was assumed that  
264 it can also be assigned to a part of the maltene fraction [108]. In the dissertation of Gaskin, it was reported that the  
265 radiolysis and not the localised heating is most probably the reason for the fibril microstructure, taking place in two  
266 steps: precipitation of paraffinic wax and diffusion of aromatics [108].

267       For the sample preparation itself, a kind of heat-casting method has been developed in [104] and was adopted  
268 in [34,109] where the bituminous samples are placed prior in covered containers about 1 hour at 110 °C, then a  
269 quantity of 0.1 grams was placed with a spatula in a cylindrical sample holder of a diameter of 8 mm and height of  
270 2 mm. Then the sample holder is placed on a heating plate for 10-30 seconds (depending on the ageing state) at  
271 150 °C to ensure flattening of the surface. The prepared samples are suggested to be stored for 24 hours at 7-8 °C  
272 before the ESEM analysis.

273



274 **4.2.3. Ageing-induced microstructure**

275 Until now ESEM observations for the changes in bitumen microstructure upon ageing are rather limited compared  
 276 to the wider use of AFM. Nevertheless, this review suggests that even these few works, provided in Table 2, report  
 277 a consistent evolution of the captured fibril network with oxidation. More specifically, the studies so far support  
 278 that the fibril network formation time is increasing with ageing [104,105,108–112], whereas it was observed that  
 279 this three-dimensional network is becoming also denser and coarser [104–107,109–111]. Processing of the ESEM  
 280 images in aged bituminous samples also showed that the fibril size (area, diameter, length) varies differently based  
 281 on the examined bitumen which can either increase [106,107,112] or decrease [104,105,108–111]. More extensive  
 282 research is needed in the near future for the effect of ageing in modified bitumens with thermosets or crumb rubber  
 283 [113]. Finally, these studies reported the association of the heavier SARA fractions with the fibril ESEM  
 284 microstructure [106,108,112].

285 Table 2: Summary of previous works with regard to ESEM bitumen observations with ageing.

Research work	Bitumen information	Ageing treatment	ESEM conditions	Testing temperature	Key conclusions
[107]	Three modified binders : SBS, styrene-ethylene-butylene-styrene (SEBS) and styrene-butylene-rubber (SBR)	TFOT at 163 °C up to 5 hours	Chamber pressure: 2.0 torr water vapor, 20keV acceleration voltage, 250x magnification	25 °C	<ul style="list-style-type: none"> <li>▪ A three-dimensional entangled network was observed in both the unaged and aged bituminous films after several minutes in beam exposure</li> <li>▪ The fibril network became coarser with ageing</li> <li>▪ The fibril diameter increased with ageing</li> </ul>
[109–111]	Four bitumens of different crude sources of similar penetration grade and softening point.	RTFOT at 123 and 163 °C followed by standard PAV	Chamber pressure: 0.8 mbar in low vacuum, 20keV acceleration voltage, 1000x magnification	Room temperature	<ul style="list-style-type: none"> <li>▪ RTFOT at 123 °C did not provoke any fibril evolution, while at 163 °C caused a denser structure</li> <li>▪ The fibril microstructure became highly denser with PAV</li> <li>▪ The fibril diameter was getting smaller with PAV for the three bitumens</li> <li>▪ The fibril formation time with ESEM irradiation increased with ageing</li> <li>▪ The fibril density increased with RTFOT</li> <li>▪ The fibril area and formation time correlated well with changes in physical properties</li> </ul>
[106]	One conventional and one SBS modified bitumen	Standard RTFOT and PAV	Chamber pressure: 0.6 torr, 20keV acceleration voltage	Not specified	<ul style="list-style-type: none"> <li>▪ The random fibril (string-like) network was assigned to the heavier molecular SARA fractions of resins and asphaltenes</li> <li>▪ The fibril network structures became coarser with increasing ageing</li> </ul>

					<ul style="list-style-type: none"> <li>▪ The fibril diameter increased by 50% with RTFOT and decreased significantly with PAV</li> <li>▪ The packing density (the distance of adjacent fibrils) increased with the ageing severity</li> </ul>
[112]	Two modified bitumens: one SBS and one SEBS	TFOT followed by standard PAV	Water vapor atmosphere of 1 to 20 torr	Room temperature	<ul style="list-style-type: none"> <li>▪ A highly entangled three-dimensional network was observed for all the bitumens</li> <li>▪ The network structure was hypothesized to appear due to evaporation of the lighter molecular oil phase</li> <li>▪ The aged bitumen appeared a less defined and entangled network</li> <li>▪ The network formation time was 5-10 times longer in the aged sample</li> <li>▪ The network chains (17 to 20 <math>\mu\text{m}</math>) was slightly higher in the aged samples</li> </ul>
[113]	Crumb rubber modified asphalt (CRMA) binder (10% crumb rubber w/w)	Standard RTFOT and PAV	Chamber pressure: 40 Pa 5-10keV acceleration voltage, up to 2000x magnification	Room temperature	<ul style="list-style-type: none"> <li>▪ Unaged CRMA binder presented a single-phase continuous non-uniform structure</li> <li>▪ The aged CRMA binder appeared two phases; a broad dark region and a lighter one attributed to the rubber-bitumen interaction</li> </ul>
[108]	Two bitumens with different asphaltene fraction percentages	Standard RTFOT and PAV	Chamber pressure: 0.6-1.4 torr water vapor, 5 to 10keV acceleration voltage, high magnification	40 °C	<ul style="list-style-type: none"> <li>▪ Ageing decreased the fibril diameter of the low asphaltene binder</li> <li>▪ The fibril structure was considered a combination of the lighter maltenes and asphaltene SARA fractions</li> <li>▪ The network formation appeared more quickly in higher testing temperatures</li> </ul>
[105]	Bitumen PG 58-28	Oxidised with lab-scale air bower at 260°C for 5 hours	Chamber pressure: 0.8 mbar in low vacuum,, 20keV acceleration voltage, 1000x magnification	Various testing temperatures	<ul style="list-style-type: none"> <li>▪ Ageing doubled the network formation time compared to the unaged bitumen</li> <li>▪ The fibrils decreased in size and increased in number with ageing, resulting in a tighter and organized microstructure</li> <li>▪ Oxidised bitumen, stored priorly at 7 °C for 14 days, appeared an intermediate micelle-like structure associated with the AFM 'bee' structures</li> </ul>
[104]	Bitumen PG 58-28, and three blends of 25, 50 and 75% of the same bitumen oxidised with PG 58-28 as base bitumen	Oxidised with lab-scale air bower at 260°C for 5 hours	Chamber pressure: 0.8 mbar in low vacuum,, 20keV acceleration voltage, 1000x magnification	Room temperature	<ul style="list-style-type: none"> <li>▪ Ageing increased the fibril network formation time</li> <li>▪ The structure was more dense and stable, with more fibril interconnections in terms of number upon ageing</li> <li>▪ The average fibril diameter decreased with oxidation</li> </ul>

## 286 **4.3. CLSM**

### 287 **4.3.1. Working principles**

288 The confocal laser scanning microscopy (CLSM) has become a popular method in biology, biomedical, and  
289 material sciences in the past few decades [114,115]. The basic concept of confocal microscopy was first developed  
290 and patented by Marvin Minsky in 1957 to image the neural networks in unstrained preparations of brain  
291 tissues [116]. Unlike conventional optical microscopes, confocal microscopes focus the light on a specific depth  
292 and eliminate any information away from the focal plane, using a spatial pinhole in front of a detector. It was during  
293 the 70s and 80s that the advances in computer and laser technology led to the development of the CLSM [117]. In  
294 CLSM, the light source, which is a laser beam, based on depth selectivity allows for optical sectioning. The  
295 information gained from this focal point is projected on a pinhole in front of the detector, which ensures that only  
296 the light from the small area of the sample, which is irradiated, is detected [118]. Apart from the reflectance or  
297 transmission mode, CLSM can also operate in fluorescence mode. This is done by using a different laser light  
298 source with a lower wavelength. In fluorescence mode, the molecules absorb the high energy (short wavelength)  
299 light and after a short lag period (fluorescence lifetime) emit a lower energy (longer wavelength) light.

300 Comparison of images taken by conventional optical microscopy and CLSM in reflected light mode has  
301 indicated the higher resolution and thus the better quality of the images obtained with CLSM [119]. Finally, in a  
302 CLSM, the image is created by scanning the surface point by point. If this is done in the x-y plane for different  
303 depths in z-direction, the 2D-images can be reconstructed to a 3D-representation, which is the biggest advantage  
304 of CLSM over other microscopy techniques [119].

### 305 **4.3.2. Bitumen application**

306 CLSM is a relatively new technique to investigate the microstructure of bitumen. This technique has been used  
307 both in reflectance and fluorescence mode on bitumen. Next to its capability of creating 3D-reconstructions, using  
308 CLSM to investigate bitumen requires little pre-treatment. This is in favor of the obtained results since changes in  
309 temperature or chemical composition may cause shifts in the molecular structure of the sample, which could lead  
310 to differences in the observed microstructures [120].

311 To prepare the bitumen samples, the general process used by researchers is as follows: the bitumen is heated  
312 between 120-160°C, then a small drop is placed on the microscope slide. A coverslip is placed onto the drop, and  
313 the sample is heated further until the top slide can be pressed against the bottom slide. The second heating period  
314 causes the drop to form a very thin film. Then the sample is kept at room temperature and atmospheric pressure so  
315 that it can cool down before placing it under the microscope [120]. The comparison of obtained images, between  
316 tests on a thin sample squeezed between two slides and a thick sample in a metal cup covered with glass, can be  
317 found in [59]. In this research, it was observed that the sizes of the crystals are larger for the thicker samples.  
318 Therefore, it was concluded that the thicker samples in metal cups are more representative of bitumen in bulk, and  
319 this procedure was recommended for observation of the wax morphology using CLSM.

320 For observations on epoxy asphalt rubbers, a different sample preparation procedure has been used. In this case,  
321 the sample is dissolved in a solvent, and the solution is spin-coated onto a microscopic slide with a speed of 3000  
322 rpm for 1 min. Afterwards, the slide is heated at around 110-115°C for 3 min to evaporate the solvent, and a cover  
323 slide is placed on top [121].

324 CLSM in reflected mode has been used by researchers to determine the size, distribution, and shape of the  
325 asphaltene particles [119] or classification of wax morphology [59]. Furthermore, in the last few years, researchers  
326 started to use this technique to observe fluorescence centers in bitumen. It was demonstrated that bitumen exhibits  
327 fluorescence when irradiated with 488 nm wavelength light [122]. Therefore, to investigate bitumen using CLSM  
328 in fluorescence mode, the samples are typically irradiated with 488 nm wavelength laser light, while observation  
329 of emitted signals is mostly done in the 500-550 nm wavelength range [120,123,124].

330 The origin of fluorescence centers in bitumen has been the subject of debate among researchers, and the  
331 conclusions over the nature of these fluorescent centers were somewhat contradictory in different  
332 articles [119,120,125]. Li & Wan found that asphaltene gives strong fluorescence when studied by CLSM. They  
333 allocate this observation to the highly conjugated aromatic structures that are a major part of asphaltene  
334 composition. It should be noted that in this study, they have separated the asphaltene fraction from the original  
335 bitumen sample by dissolving the bitumen sample in n-heptane. This precipitation process could influence the  
336 structure of the molecules, hence it is a distinct possibility that their results have been compromised [119].

337 A study of fluorescence signals in bitumen was also conducted by Bearsley and his group. In this study, the bee-  
338 like structures, observed with AFM, and the fluorescent particles, observed with CLSM, were both of the same  
339 dimensions. The geometrical similarities cause a presumption of the latter being asphaltenes. To verify this  
340 hypothesis, separation of asphaltene and maltene fractions was done according to ASTM D4124-01 (2002). When  
341 both major phases were evaluated using CLSM, asphaltenes seemed to exhibit a uniform fluorescence signal. For  
342 this reason, they concluded that asphaltene is in fact, the cause of the fluorescence signals in bitumen [120].

343 However, Handle and his peers showed that the aromatic mantle, serving as a stabilizing agent around the  
344 micelle, is responsible for the high-intensity fluorescent emissions in the visible range and not the asphaltenes  
345 themselves. To prove their hypothesis that asphaltenes are incapable of producing fluorescence and the  
346 fluorescence signals come from the maltene phase, they studied the different bitumen fractions separately. They  
347 observed that asphaltenes emit barely any fluorescent signals, and maltenes, on the other hand, produce very strong  
348 signals. By fractioning the maltene phase, they found the aromatics to be the most fluorescent fraction. However,  
349 they did not neglect the similarities with the bee-like structures by comparing their conclusions on the source of  
350 fluorescence and the micelle theory. Interestingly, they stated that the fluorescence signals are still derived from  
351 the asphaltene micelles, however not from the inner core, as presumed previously, but from a surrounding mantle  
352 of aromatics [125–127].

353 Other than using CLSM to investigate virgin bitumen, this technique was also used to study the morphology of  
354 polymer modified bitumen [107,128,129] and recycled asphalt shingle blended with asphalt binder [123].  
355 Moreover, CLSM has been widely used to explore the morphology of epoxy asphalt binder [130], phase-separated  
356 microstructure and dispersion of the asphalt rubber in epoxy asphalt [121,131], as well as morphology and phase  
357 separation of polymer-modified epoxy asphalt binders [132–134].

#### 358 ***4.3.3. Ageing-induced microstructure***

359 Up until now, only a few researchers have used CLSM to investigate the microstructure of bitumen upon ageing.  
360 Most of these studies use CLSM in fluorescence mode, to observe the fluorescence centers and propose ageing  
361 models by relating these centers to different fractions of bitumen.

362 Großegger used CLSM to investigate ageing of bitumen, discovering fluorescence centers in both unaged and  
363 laboratory aged samples. The sizes of the centers in both samples were in the same range of 1 to 2  $\mu\text{m}$ , and apart

364 from the induced artefacts at the edges of the images, the fluorescence centers remained constant [124]. These  
 365 findings are in-line with the observations of Bearsley in which the structure and fluorescence of the asphaltene  
 366 phase did not alter radically upon ageing [120].

367 However, these conclusions were in contrast with the research previously done by Li & Wan [119]. Their research  
 368 with CLSM on asphaltenes showed that the fluorescence almost vanishes after 48 hours from the time when the  
 369 sample is exposed to air. However, when the sample was kept in a dry box filled with nitrogen, the fluorescence  
 370 signal stayed invariable. They concluded that the difference in evolution due to ageing could be a consequence of  
 371 numerous factors, including oxidation. Possible explanations for these contradictions between studies can be found  
 372 in the difference in temperature or time passed between the preparation of the sample and performing the test.  
 373 Furthermore, an important factor that could have influenced the results is the difference in the studied samples.

374 In more recent research, Handle and his colleagues proved the existence of two separate phases in bitumen using  
 375 CLSM and proposed an enhanced micelle theory for ageing of bitumen that can explain the different effects of  
 376 short- and long-term ageing, as well as healing due to temperature elevation [125]. In another study, CLSM was  
 377 used to investigate the ageing properties of PMB by measuring the fluorescence emission of the samples. The  
 378 results showed a decreased fluorescence intensity for the aged samples compared with unaged samples [129].

379 A list of different studies using CLSM to investigate the ageing of bitumen is presented in Table 3. Most of these  
 380 studies use CLSM in fluorescence mode or conduct measurements with a lower resolution than AFM. However,  
 381 since recently developed CLSMs can acquire images with the same resolution as AFM, further studies in this field  
 382 are still needed.

383 Table 3: Summary of previous works with regard to CLSM bitumen observations with ageing.

Research work	Bitumen information	Ageing treatment	CLSM mode	Testing temperature	Key conclusions
[120]	Two bitumens obtained from a Saudi Arabian, Safaniyan crude with penetration grades of 180/200 and 80/100. A third bitumen, AR4000 viscosity graded bitumen manufactured from a Californian, San Joaquin crude.	Artificially aged as 1 mm films in a forced draft convection oven at $60 \pm 2$ °C for $3024 \pm 8$ h.	Fluorescence mode	Room temperature	<ul style="list-style-type: none"> <li>▪ Possibility to observe the asphaltene phase of bitumen</li> <li>▪ Fluorescence is influenced by the chemical nature of the bitumen. Therefore optimum conditions for observing bitumen of different sources could vary</li> <li>▪ The observed structure does not change significantly upon ageing</li> </ul>

[135]	Unmodified 70/100 pen bitumen.	RTFOT, RTFOT + PAS, exposure in road	Fluorescence mode	Not specified	<ul style="list-style-type: none"> <li>The spatial distribution, size and shape of the fluorescence centers vary with origin, treatment state and ageing.</li> </ul>
[124]	Unmodified 70/100 pen bitumen.	Standard PAV	Transmission and fluorescence mode	Room temperature	<ul style="list-style-type: none"> <li>Observation of typical fluorescence centers on both unaged and aged bitumen samples.</li> <li>The centers were evenly distributed and in the same range of 1 to 2 <math>\mu\text{m}</math> for both aged and unaged samples.</li> </ul>
[119]	Cold lake bitumen samples with n-pentane insoluble asphaltene content of 17.8%.	Exposure to air for 24-48 h.	Reflected light and fluorescence mode	24-48 hours exposure to air & two weeks under dry nitrogen atmosphere inside a box.	<ul style="list-style-type: none"> <li>Fluorescence on asphaltene samples almost vanishes after 48 hours from the time the sample is exposed to air.</li> <li>Fluorescence on asphaltene samples remains the same when the sample is kept in a dry box filled with nitrogen</li> </ul>
[125]	Five samples were used: A typical 50/70 bitumen, two SBS-modified bitumen produced from a 70/100 bitumen, precursor sample 1 (vacuum flashed, cracked residuum), and precursor sample 2 (residuum of vacuum distillation)	No ageing treatment	Fluorescence mode	Room temperature	<ul style="list-style-type: none"> <li>Observation of two separate phases in bitumen, as predicted by the micelle theory.</li> <li>Development of an enhanced micelle theory for ageing, capable of explaining the different effects of short term and long term ageing as well as thermal healing of asphalt concrete.</li> </ul>
[129]	SBS block copolymer modified bitumen	Standard PAV	Fluorescence mode	Room temperature	<ul style="list-style-type: none"> <li>Phase morphology of PMB samples alter depending on the mixing time and/or shear rate applied.</li> <li>Shear rate is more influential than mixing time in achieving a highly dispersed SBS phase in bitumen.</li> <li>Ageing of PMB samples caused a decrease in fluorescence intensity.</li> </ul>

### 384 5. Comparative overview for bitumen application

385 In this research, the application of three microscopic techniques to analyse the obtained microstructural changes  
386 upon oxidative ageing of bitumen was reviewed. The summary of the main information of these commonly used  
387 instruments for these observations is presented in Table 4. Each instrument has its own advantages and limitations,  
388 which means that the choice of microscopy is dependent on which microstructural characteristics and degree of  
389 detail is required as well as the possession and costs of such a microscope, especially in small-scale laboratories.

390 Table 4: Comparison of the three microscopies for bitumen application.

Microscope	Radiation source	Working medium	Specimen mounting	Best resolution	Cost of equipment
AFM	Micro cantilever probe	air	Aluminum stubs or glass slides	0.5 nm	++
ESEM	Electrons	gaseous environment	Cylindrical sample holder	1.3 nm	+++
CLSM	Laser light	air	Glass slide	1 nm	++

391

392 **5.1. Limitations and advantages**

393 There is a wide range of microscopic imaging techniques available to evaluate the microstructure of bitumen.  
394 Currently, AFM is the most common instrument used to investigate the ageing phenomenon in bituminous binders.  
395 AFM requires minimum sample preparation, can operate in ambient conditions and provides better resolution than  
396 ESEM. Other than the microstructure, AFM is also able to provide information on the mechanical properties of the  
397 sample in nanoscale. However, this method is highly sensitive to vibrations during the measurements, can only  
398 conduct measurements on a limited scanning area, and has limitations while conducting measurements on material  
399 with high viscosity or large height differences.

400 Another popular instrument to examine the effect of ageing on bitumen is ESEM. This microscope is designed  
401 based on SEM but permits measurements in a near ambient environment in which the sample does not need to be  
402 coated with gold or carbon, and there is no need to have a high vacuum in the sample chamber. Even though this  
403 feature makes measurements on bitumen samples possible, ESEM is still not favored by many researchers to  
404 observe the bitumen microstructure. This is due to the fact that the fibril network observed on the surface of the  
405 samples by ESEM is caused by the microscope itself after several minutes of electron beam exposure and does not  
406 correspond with the observations of other microscopic techniques.

407 A rather recent microscopic technique used by researchers to investigate the ageing of bitumen is CLSM. By using  
408 these instruments in fluorescence mode, it is possible to observe the fluorescence centers on the surface of the  
409 samples and further improve the available ageing models. The application of CLSM on bitumen in the literature is  
410 mostly limited to fluorescence imaging. However, the exceptional resolution (as low as 1 nm in ideal conditions)



411 of the recently developed commercial CLSMs in reflection mode, which are comparable with the resolution of  
412 AFM, provides an opportunity to observe the detailed microstructure of bitumen in future research. Furthermore,  
413 in contrast to AFM, the multi-focus imaging capability of the CLSM makes acquiring non-contact images of non-  
414 smooth surfaces with large height differences possible. Another advantage of CLSM that has not been fully  
415 employed in this field is its ability to map the 3D surfaces and produce images of a sample in multiple scales. These  
416 abilities, combined with some advanced image processing techniques, can lead to a detailed analysis of a time-  
417 dependent phenomenon such as ageing.

## 418 **5.2. Need for a common preparation protocol**

419 Sample preparation is a crucial step before acquiring images with any microscope. The microstructural properties  
420 of bitumen are strongly dependent on the temperature when the sample is extracted, isothermal annealing, and  
421 cooling rate. The sample preparation method is important since bitumen can age or undergo steric hardening during  
422 or after the sample preparation stage, so that the examined sample might not be a good representation of the bulk  
423 material, or bitumen samples might collect dust particles before the images are acquired. Various preparation  
424 methods have been developed and used by researchers, but a standard method has not yet been established to  
425 investigate the microstructure of bitumen using the microscopes reviewed in this article. Comparison between  
426 different sample preparation methods on the morphological properties of polymer modified bitumen samples using  
427 fluorescence microscopy is available in [129,130].

428 The most common sample preparation method used in the literature that is recommended by the authors is as  
429 follows:

- 430 I. The preparation should start with a high-temperature treatment to create a workable and homogenous  
431 material. The temperature and heating time are chosen based on bitumen type and ageing state and is  
432 often between 110 and 160 °C. Even though higher temperature have also been used in the literature, this  
433 can cause additional ageing in the material and is not recommended.
- 434 II. A sample holder (microscopic slide) is placed horizontally on a heating plate set at temperature 140-  
435 160 °C. A bitumen drop is placed on the sample holder and left until a smooth surface (1-2 minutes) with  
436 sufficient thickness is obtained.
- 437 III. The sample is left inside a dust-free environment for two hours to cool down to the ambient temperature.  
438 If applicable, the cooling rate is kept between 2 °C/min and 3.4 °C/min to obtain similar cooling  
439 conditions of bitumen during asphalt mixture compaction.
- 440 IV. Finally, images can be taken at different time intervals, using a non-contact microscopic technique, to  
441 keep the surface of the samples free of any artefacts.

## 442 **6. Conclusions and recommendations**

443 The conclusions that have been extracted by the present literature review for the three most promising  
444 microscopic techniques with respect to ageing of bituminous binders are summarised herein:

- 445
- 446     ▪ There is a transition from the classic colloidal theory of bitumen's microstructure to an asphaltene  
447 nanoaggregation model.
  - 448     ▪ There is still controversy about the source of commonly observed microstructural patterns. The wax  
449 crystallisation gains recently more acceptance against the belief of asphaltenes being the source of certain  
450 microstructures.
  - 451     ▪ AFM is the most widely utilised microscopy to capture changes in bitumen microstructure with ageing.  
452 Typical bee-like structures are captured with AFM which either increase or decrease with short- and long-  
453 term laboratory ageing in terms of average size, based on the used binder.
  - 454     ▪ ESEM is capable of imaging fibril-like microstructural patterns in bituminous samples. This fibril network  
455 is getting denser and coarser with ageing, while its formation time is increasing. A clear association of  
456 ageing with changing trend (increasing or decreasing) of fibril size is not possible based on the existed  
457 literature.
  - 458     ▪ CLSM has been utilised to capture the fluorescent centres in the different bitumen fractions. Fluorescent  
459 centres have been linked with the asphaltenes' fraction in bitumen. They have been reported to be either  
460 unaffected in terms of size by ageing or to disappear upon oxidation.
  - 461     ▪ Based on a comparative analysis, the future of microscopy in small-scale asphalt laboratories seems to  
462 belong to CLSM since CLSM in reflection mode is rather underutilized and can offer, among others,  
463 imaging of high resolution and mapping in 3D surfaces.
  - 464     ▪ A simplistic common preparation procedure for bituminous microscopic samples is suggested to be adopted  
465 in order to reduce variations between different research groups.

466

467 Yet, despite the understanding of the overwhelming benefits of microscopic techniques to capture ageing-  
468 induced microstructures in bitumen, the efforts to link them with upper scales can be somehow biased when the

469 investigated binders are rather limited. Therefore it is recommended that the bitumen research community turns  
 470 towards a more systematic investigation of bituminous binders, of different origin and performance, to verify  
 471 certain trends and microstructural patterns reported upon ageing. It remains to be seen if the microstructural theories  
 472 proposed up to now will be able to explain the formation and change of these microstructural patterns with ageing.  
 473 Epitomising, it is believed that this review will consist a useful guide for the pavement engineer who is concerned  
 474 not only for the bitumen's performance but also for the reasons and links behind this.

#### 475 **Acknowledgements**

476 The authors gratefully acknowledge the constructive comments of Hilde Soenen (Nynas NV) which helped to  
 477 improve considerably the manuscript as well as the University of Antwerp for funding the AQ<sup>2</sup>UABIT (Advanced  
 478 Qualitative and QUantitative surface Analysis of BITuminous binders using laser scanning confocal microscopy)  
 479 project with the IOF-SBO research fund (project nr. 40204).

#### **References**

- [1] Eurobitume, The Bitumen Industry: A Global Perspective, 2011.
- [2] R. Maharaj, A Comparison of the Composition and Rheology of Trinidad Lake Asphalt and Trinidad, *Int. J. Appl. Chem.* 5 (2009) 169–179.
- [3] J.S. Moulthrop, M. Massoud, The SHRP Materials Reference Library, Washington DC, 1993.
- [4] X. Lu, P. Sjövall, H. Soenen, Structural and chemical analysis of bitumen using time-of-flight secondary ion mass spectrometry (TOF-SIMS), *Fuel*. 199 (2017) 206–218. <https://doi.org/10.1016/j.fuel.2017.02.090>.
- [5] G. Pipintakos, H.Y.V. Ching, H. Soenen, P. Sjövall, U. Mühlich, S. Van Doorslaer, A. Varveri, W. Van den bergh, X. Lu, Experimental investigation of the oxidative ageing mechanisms in bitumen, *Constr. Build. Mater.* 260 (2020) 119702. <https://doi.org/10.1016/j.conbuildmat.2020.119702>.
- [6] G. Tarsi, A. Varveri, C. Lantieri, A. Scarpas, C. Sangiorgi, Effects of Different Aging Methods on Chemical and Rheological Properties of Bitumen, *J. Mater. Civ. Eng.* 30 (2018). [https://doi.org/10.1061/\(asce\)mt.1943-5533.0002206](https://doi.org/10.1061/(asce)mt.1943-5533.0002206).
- [7] S. Weigel, D. Stephan, Relationships between the chemistry and the physical properties of bitumen, 0629 (2018). <https://doi.org/10.1080/14680629.2017.1338189>.
- [8] X. Lu, U. Isacson, Effect of ageing on bitumen chemistry and rheology, *Constr. Build. Mater.* 16 (2002) 15–22. [https://doi.org/10.1016/s0950-0618\(01\)00033-2](https://doi.org/10.1016/s0950-0618(01)00033-2).
- [9] A. Margaritis, H. Soenen, E. Fransen, G. Pipintakos, G. Jacobs, J. Blom, W. Van Den, Identification of ageing state clusters of reclaimed asphalt binders using principal component analysis ( PCA ) and hierarchical cluster analysis ( HCA ) based on chemo-rheological parameters, *Constr. Build. Mater.* 244 (2020) 118276. <https://doi.org/10.1016/j.conbuildmat.2020.118276>.
- [10] G. Pipintakos, H. Soenen, H.Y.V. Ching, C. Vande Velde, S. Van Doorslaer, F. Lemièrè, A. Varveri, W. Van den bergh, Exploring the oxidative mechanisms of bitumen after laboratory short- and long-term ageing, *Constr. Build. Mater.* 289 (2021) 123182. <https://doi.org/10.1016/j.conbuildmat.2021.123182>.
- [11] H. Yao, Q. Dai, Z. You, Fourier Transform Infrared Spectroscopy characterization of aging-related properties of original and nano-modified asphalt binders, *Constr. Build. Mater.* 101 (2015) 1078–1087. <https://doi.org/10.1016/j.conbuildmat.2015.10.085>.
- [12] A.A.A. Molenaar, E.T. Hagos, M.F.C. van de Ven, Effects of Aging on the Mechanical Characteristics of Bituminous Binders in PAC, *J. Mater. Civ. Eng.* 22 (2010). [https://doi.org/10.1061/\(ASCE\)MT.1943-5533.0000021](https://doi.org/10.1061/(ASCE)MT.1943-5533.0000021).

- [13] Y.R. Kim, C. Castorena, M. Elwardany, F.Y. Rad, S. Underwood, A. Gundha, P. Gudipudi, M.J. Farrar, R.R. Glaser, and, Long-Term Aging of Asphalt Mixtures for Performance Testing and Prediction, Transportation Research Board, 2017. <https://doi.org/10.17226/24959>.
- [14] F. Wang, Y. Xiao, P. Cui, J. Lin, M. Li, Z. Chen, Correlation of asphalt performance indicators and aging Degrees : A review, *Constr. Build. Mater.* 250 (2020) 118824. <https://doi.org/10.1016/j.conbuildmat.2020.118824>.
- [15] EN12607-1: Bitumen and bituminous binders. Determination of the resistance to hardening under the influence of heat and air–Part 1: RTFOT method, 2007.
- [16] EN 14769: Bitumen and Bituminous Binders. Accelerated Long-term Ageing Conditioning by a Pressure Ageing Vessel (PAV), 2012.
- [17] R. Tauste, Understanding the bitumen ageing phenomenon : A review, *Constr. Build. Mater.* 192 (2018) 593–609. <https://doi.org/10.1016/j.conbuildmat.2018.10.169>.
- [18] J.C. Petersen, A Review of the Fundamentals of Asphalt Oxidation (E-C140), *Transp. Res. Rec. J. Transp. Res. Board.* (2009). <https://doi.org/10.17226/23002>.
- [19] P.R. Herrington, Diffusion and reaction of oxygen in bitumen films, *Fuel.* 94 (2012) 86–92. <https://doi.org/10.1016/j.fuel.2011.12.021>.
- [20] J. Mirwald, S. Werkovits, I. Camargo, D. Maschauer, B. Hofko, H. Grothe, Understanding bitumen ageing by investigation of its polarity fractions, *Constr. Build. Mater.* 250 (2020) 118809. <https://doi.org/10.1016/j.conbuildmat.2020.118809>.
- [21] J.C. Petersen, R. Glaser, Asphalt Oxidation Mechanisms and the Role of Oxidation Products on Age Hardening Revisited, *Road Mater. Pavement Des.* 12 (2011) 795–819. <https://doi.org/10.1080/14680629.2011.9713895>.
- [22] M. Zhang, P. Hao, S. Dong, Y. Li, G. Yuan, Asphalt binder micro-characterization and testing approaches : A review, *Measurement.* 151 (2020) 107255. <https://doi.org/10.1016/j.measurement.2019.107255>.
- [23] B. Hofko, Influence of asphaltene content on mechanical bitumen behavior : experimental investigation and micromechanical modeling, (2014). <https://doi.org/10.1617/s11527-014-0383-7>.
- [24] M.C. Cavalli, M. Zaumanis, E. Mazza, M.N. Partl, L.D. Poulidakos, Aging effect on rheology and cracking behaviour of reclaimed binder with bio-based rejuvenators, *J. Clean. Prod.* 189 (2018) 88–97. <https://doi.org/10.1016/j.jclepro.2018.03.305>.
- [25] X. Hou, F. Xiao, J. Wang, S. Amirkhanian, Identification of asphalt aging characterization by spectrophotometry technique, *Fuel.* 226 (2018) 230–239. <https://doi.org/10.1016/j.fuel.2018.04.030>.
- [26] P.K. Das, R. Balieu, N. Kringos, B. Birgisson, On the oxidative ageing mechanism and its effect on asphalt mixtures morphology, *Mater. Struct.* 48 (2014) 3113–3127. <https://doi.org/10.1617/s11527-014-0385-5>.
- [27] A. Dony, L. Ziyani, I. Drouadaine, S. Pouget, S. Faucon-Dumont, D. Simard, V. Mouillet, J.E. Poirier, T. Gabet, L. Boulange, A. Nicolai, C. Gueit, 1, MURE National Project : FTIR spectroscopy study to assess ageing of asphalt mixtures, in: 6th Eurasphalt Eurobitume Congr., 2016. <https://doi.org/dx.doi.org/10.14311/EE.2016.154>.
- [28] J. Lamontagne, P. Dumas, V. Mouillet, J. Kister, Comparison by Fourier transform infrared ( FTIR ) spectroscopy of different ageing techniques : application to road bitumens, *Fuel.* 80 (2001) 483–488. [https://doi.org/10.1016/S0016-2361\(00\)00121-6](https://doi.org/10.1016/S0016-2361(00)00121-6).
- [29] Y. Cui, C.J. Glover, J. Braziunas, H. Sivilevicius, Further exploration of the pavement oxidation model Diffusion-reaction balance in asphalt, *Constr. Build. Mater.* 161 (2018) 132–140. <https://doi.org/10.1016/j.conbuildmat.2017.11.095>.
- [30] L.W. Corbett, R.E. Merz, Asphalt Binder Hardening in the Michigan Test Road After 18 Years of Service, *Transp. Res. Rec.* (1975) 27–34.
- [31] E. Institute, IP 469/01: Determination of saturated, aromatic and polar Flame, compounds in petroleum products by thin layer chromatography and ionization detection, 2006.
- [32] N. Sakib, A. Bhasin, N. Sakib, Measuring polarity-based distributions ( SARA ) of bitumen using simplified chromatographic techniques, *Int. J. Pavement Eng.* 8436 (2019) 1–28. <https://doi.org/10.1080/10298436.2018.1428972>.
- [33] A. Vaitkus, A. Zofka, Evaluation of bitumen fractional composition depending on the crude oil type and production technology, in: 9th Int. Conf. Environ. Eng., 2014.
- [34] P. Mikhailenko, H. Baaj, Comparison of Chemical and Microstructural Properties of Virgin and Reclaimed Asphalt Pavement Binders and Their Saturate , Aromatic , Resin , and Asphaltene Fractions, *Energy &*

- Fuels. 33 (2019) 2633–2640. <https://doi.org/10.1021/acs.energyfuels.8b03414>.
- [35] K. Zhao, Y. Wang, F. Li, Influence of ageing conditions on the chemical property changes of asphalt binders, *Road Mater. Pavement Des.* (2019) 1–29. <https://doi.org/10.1080/14680629.2019.1637771>.
- [36] U. Mühlich, G. Pipintakos, C. Tsakalidis, Mechanism based diffusion-reaction modelling for predicting the influence of SARA composition and ageing stage on spurt completion time and diffusivity in bitumen, *Constr. Build. Mater.* (2020) 120592. <https://doi.org/10.1016/j.conbuildmat.2020.120592>.
- [37] D. Lesueur, The colloidal structure of bitumen: Consequences on the rheology and on the mechanisms of bitumen modification, *Adv. Colloid Interface Sci.* 145 (2009) 42–82. <https://doi.org/10.1016/j.cis.2008.08.011>.
- [38] P. Redelius, H. Soenen, Relation between bitumen chemistry and performance, *Fuel*. 140 (2015) 34–43. <https://doi.org/10.1016/j.fuel.2014.09.044>.
- [39] D. Lesueur, Evidence of the Colloidal Structure of Bitumen, in: *ISAP Int. Work. Chemo-Mechanics Bitum. Mater.*, 2009. <https://doi.org/10.1016/j.cis.2008.08.011>.
- [40] J.C. Petersen, R.E. Robertson, J.F. Branthaver, P.M. Harnsberger, J.J. Duvall, S.S. Kim, D.A. Anderson, D.W. Christiansen, H.U. Bahia, Binder characterization and evaluation: Volume 1, Rep. No. SHRP-A-367, *Strateg. Highw. Res. Program, Natl. Res. Council*. Washington, DC. (1994).
- [41] P.G. Redelius, The structure of asphaltenes in bitumen, *Road Mater. Pavement Des.* 7 (2006) 143–162. <https://doi.org/10.1080/14680629.2006.9690062>.
- [42] E. Iskender, Evaluation of mechanical properties of nano-clay modified asphalt mixtures, *Measurement*. 93 (2016) 359–371. <https://doi.org/10.1016/j.measurement.2016.07.045>.
- [43] A. Rosinger, Beiträge zur Kolloidchemie des Asphalts, *Kolloid-Zeitschrift*. 15 (1914) 177–179. <https://doi.org/10.1007/BF01427821>.
- [44] F.J. Nellensteyn, The constitution of asphalt, *J. Inst. Pet. Technol.* 10 (1924) 311–323.
- [45] J.M. Swanson, A Contribution to the Physical Chemistry of the Asphalts., *J. Phys. Chem.* 46 (1942) 141–150.
- [46] J.P. Pfeiffer, R.N.J. Saal, Asphaltic bitumen as colloid system., *J. Phys. Chem.* 44 (1940) 139–149.
- [47] J.P. Pfeiffer, The properties of asphaltic bitumen, (1950).
- [48] C. Gaestel, R. Smadja, K.A. Lamminan, Contribution à la connaissance des propriétés des bitumes routiers, *Rev. Gentile. Routes Aérodromes*. 466 (1971) 85–94.
- [49] M. Paliukaite, A. Vaitkus, A. Zofka, Evaluation of bitumen fractional composition depending on the crude oil type and production technology, in: 2014. <https://doi.org/10.3846/enviro.2014.162>.
- [50] D. Christensen, DW Anderson, Rheological evidence concerning the molecular architecture of asphalt cements., in: *Proc. Chem. Bitumen, Vol 2, Rome, Pp.*, 1991: pp. 568–95.
- [51] B. Schuler, Y. Zhang, F. Liu, A.E. Pomerantz, A. Ballard, L. Gross, V. Pauchard, S. Banerjee, O.C. Mullins, Overview of Asphaltene Nanostructures and Thermodynamic Applications, (2020). <https://doi.org/10.1021/acs.energyfuels.0c00874>.
- [52] O.C. Mullins, The Modified Yen Model †, (2010) 2179–2207. <https://doi.org/10.1021/ef900975e>.
- [53] O.C. Mullins, H. Sabbah, A.E. Pomerantz, A.B. Andrews, Y. Ruiz-morales, F. Mostow, R. Mcfarlane, L. Goual, R. Lepkowicz, T. Cooper, J. Orbulescu, R.M. Leblanc, J. Edwards, R.N. Zare, Advances in Asphaltene Science and the Yen – Mullins Model, (2012). <https://doi.org/https://doi.org/10.1021/ef300185p>.
- [54] J. Eyssautier, P. Levitz, D. Espinat, J. Jestin, I. Grillo, L. Barr, Insight into Asphaltene Nanoaggregate Structure Inferred by Small Angle Neutron and X-ray Scattering, (2011) 6827–6837. <https://doi.org/https://doi.org/10.1021/jp111468d>.
- [55] R.D. Majumdar, T. Montana, O.C. Mullins, M. Gerken, P. Hazendonk, Insights into asphaltene aggregate structure using ultrafast MAS solid-state <sup>1</sup>H NMR spectroscopy, *Fuel*. 193 (2017) 359–368. <https://doi.org/10.1016/j.fuel.2016.12.082>.
- [56] X. Lu, P. Redelius, Compositional and Structural Characterization of Waxes Isolated from Bitumens, *Energy & Fuels*. 20 (2006) 653–660. <https://doi.org/10.1021/ef0503414>.
- [57] L. Carbognani, L. DeLima, M. Orea, U. Ehrmann, STUDIES ON LARGE CRUDE OIL ALKANES. II. ISOLATION AND CHARACTERIZATION OF AROMATIC WAXES AND WAXY ASPHALTENES., *Pet. Sci. Technol.* 18 (2000) 607–634. <https://doi.org/10.1080/10916460008949863>.
- [58] M. Djabourov, J. Volle, M. Kane, J. Lechaire, G. Frebourg, Morphology of paraffin crystals in waxy crude oils cooled in quiescent conditions and under flow, 82 (2003) 127–135. <https://doi.org/10.1016/S0016->

- 2361(02)00222-3.
- [59] X. Lu, M. Langton, P. Olofsson, P. Redelius, Wax morphology in bitumen, *J. Mater. Sci.* 40 (2005) 1893–1900. <https://doi.org/10.1007/s10853-005-1208-4>.
- [60] P. Claudy, G.N. King, Caractérisation des bitumes routiers par analyse calorimétrique différentielle (ACD). Analyse thermo-optique (ATO). Corrélation entre propriétés physiques et résultats ACD, *Bull. Liaison Des Lab. Des Ponts Chaussees.* (1992).
- [61] P. Claudy, J.M. Letoffe, G.N. King, J.P. Plancke, Characterization of asphalts cements by thermomicroscopy and differential scanning calorimetry: correlation to classic physical properties, *Fuel Sci. Technol. Int.* 10 (1992) 735–765. <https://doi.org/10.1080/08843759208916019>.
- [62] H.U. Bahia, D.A. Anderson, D.W. Christensen, The bending beam rheometer; a simple device for measuring low-temperature rheology of asphalt binders (with discussion), *J. Assoc. Asph. Paving Technol.* 61 (1992).
- [63] H. Soenen, A. Vanelstraete, Influence of thermal history on rheological properties of various bitumen, (2006) 729–739. <https://doi.org/10.1007/s00397-005-0032-8>.
- [64] G. Binnig, C.F. Quate, C. Gerbe, Atomic Force Microscope, *Phys. Rev. Lett.* 56 (1986).
- [65] P.K. Das, H. Baaj, S. Tighe, N. Kringos, Atomic force microscopy to investigate asphalt binders : a state-of-the-art review, 0629 (2015). <https://doi.org/10.1080/14680629.2015.1114012>.
- [66] L. Loeber, O. Sutton, J. Morel, J. Valleton, G. Muller, New direct observations of asphalts and asphalt binders by scanning electron microscopy and atomic force microscopy, 182 (1996) 32–39. <https://doi.org/10.1046/j.1365-2818.1996.134416.x>.
- [67] V. Bellitto, Atomic force microscopy: imaging, measuring and manipulating surfaces at the atomic scale, *BoD–Books on Demand*, 2012. <https://doi.org/10.5772/2673>.
- [68] J. Aguiar-moya, J.A. Salazar-delgado, A. García, J.P. Aguiar-moya, J. Salazar-delgado, A. Baldi-, L.G. Loria-salazar, A. García, J.P. Aguiar-moya, J. Salazar-delgado, Methodology for estimating the modulus of elasticity of bitumen under different aging conditions by AFM, *Road Mater. Pavement Des.* (2019). <https://doi.org/10.1080/14680629.2019.1588152>.
- [69] H. Ban, P. Karki, Y.-R. Kim, Nanoindentation test integrated with numerical simulation to characterize mechanical properties of rock materials, *J. Test. Eval.* 42 (2014) 787–796. <https://doi.org/10.1520/JTE20130035>.
- [70] J. Blom, H. Soenen, A. Katsiki, N. Van Den Brande, H. Rahier, Investigation of the bulk and surface microstructure of bitumen by atomic force microscopy, *Constr. Build. Mater.* 177 (2020) 158–169. <https://doi.org/10.1016/j.conbuildmat.2018.05.062>.
- [71] H.R. Fischer, E.C. Dillingh, C.G.M. Hermse, Applied Surface Science On the interfacial interaction between bituminous binders and mineral surfaces as present in asphalt mixtures, *Appl. Surf. Sci.* 265 (2013) 495–499. <https://doi.org/10.1016/j.apsusc.2012.11.034>.
- [72] S.N. Nahar, A.J.M. Schmets, C. Kasbergen, G. Schitter, A. Scarpas, Self-healing of bituminous materials by damage reversal at the microstructural scale, in: *Proc. 94th Annu. Meet. Transp. Res. Board*, 2015: pp. 11–15.
- [73] R.G. Allen, D.N. Little, D.M. Asce, A. Bhasin, Structural Characterization of Micromechanical Properties in Asphalt Using Atomic Force Microscopy, 24 (2012) 1317–1327. [https://doi.org/10.1061/\(ASCE\)MT.1943-5533.0000510](https://doi.org/10.1061/(ASCE)MT.1943-5533.0000510).
- [74] H. Soenen, J. Besamusca, H.R. Fischer, L.D. Poulikakos, J. Planche, P.K. Das, Laboratory investigation of bitumen based on round robin DSC and AFM tests, (2014). <https://doi.org/10.1617/s11527-013-0123-4>.
- [75] J. Masson, V. Leblond, J. Margeson, Bitumen morphologies by phase-detection atomic force microscopy, *J. Microsc.* 221 (2006) 17–29. <https://doi.org/10.1111/j.1365-2818.2006.01540.x>.
- [76] A. Jäger, R. Lackner, C. Eisenmenger-Sittner, R. Blab, Identification of four material phases in bitumen by atomic force microscopy, *Road Mater. Pavement Des.* 5 (2004) 9–24. <https://doi.org/10.1080/14680629.2004.9689985>.
- [77] A.T. Pauli, R.E. Robertson, C.M. Eggleston, J.F. Branthaver, W. Grimes, Atomic force microscopy investigation of SHRP asphalts, *Prepr. Chem. Soc. Div. Pet. Chem.* 46 (2001) 104–110.
- [78] H. Fischer, L.D. Poulikakos, J.-P. Planche, P. Das, J. Grenfell, Challenges While Performing AFM on Bitumen, in: N. Kringos, B. Birgisson, D. Frost, L. Wang (Eds.), *Multi-Scale Model. Charact. Infrastruct. Mater.*, Springer Netherlands, Dordrecht, 2013: pp. 89–98. [https://doi.org/10.1007/978-94-007-6878-9\\_7](https://doi.org/10.1007/978-94-007-6878-9_7).
- [79] P.K. Das, N. Kringos, V. Wallqvist, B. Birgisson, Micromechanical investigation of phase separation in

- bitumen by combining atomic force microscopy with differential scanning calorimetry results, *Road Mater. Pavement Des.* 14 (2013) 25–37. <https://doi.org/10.1080/14680629.2013.774744>.
- [80] H.R. Fischer, A. Cernescu, Relation of chemical composition to asphalt microstructure – Details and properties of micro-structures in bitumen as seen by thermal and friction force microscopy and by scanning near-field optical microscopy, *Fuel*. 153 (2015) 628–633. <https://doi.org/10.1016/j.fuel.2015.03.043>.
- [81] T. Pauli, W. Grimes, A. Cookman, S.-C. Huang, Adherence energy of asphalt thin films measured by force-displacement atomic force microscopy, *J. Mater. Civ. Eng.* 26 (2014) 4014089. [https://doi.org/10.1061/\(ASCE\)MT.1943-5533.0001003](https://doi.org/10.1061/(ASCE)MT.1943-5533.0001003).
- [82] Å.L. Lyne, V. Wallqvist, M.W. Rutland, P. Claesson, B. Birgisson, Surface wrinkling: the phenomenon causing bees in bitumen, *J. Mater. Sci.* 48 (2013) 6970–6976. <https://doi.org/10.1007/s10853-013-7505-4>.
- [83] A. Ramm, M.C. Downer, N. Sakib, A. Bhasin, Morphology and kinetics of asphalt binder microstructure at gas, liquid and solid interfaces., *J. Microsc.* 276 (2019) 109–117. <https://doi.org/10.1111/jmi.12842>.
- [84] A. Ramm, N. Sakib, A. Bhasin, M.C. Downer, Optical characterization of temperature- and composition-dependent microstructure in asphalt binders, *J. Microsc.* 262 (2016) 216–225. <https://doi.org/https://doi.org/10.1111/jmi.12353>.
- [85] J.P. Aguiar-moya, J. Salazar-delgado, A. García, A. Baldi-, V. Bonilla-mora, L.G. Loría-salazar, J. Salazar-delgado, A. García, A. Baldi-, Effect of ageing on micromechanical properties of bitumen by means of atomic force microscopy, *Road Mater. Pavement Des.* 18 (2017) 203–215. <https://doi.org/10.1080/14680629.2017.1304249>.
- [86] S. Liu, A. Peng, S. Zhou, J. Wu, W. Xuan, W. Liu, Evaluation of the ageing behaviour of waste engine oil-modified asphalt binders, *Constr. Build. Mater.* 223 (2019) 394–408. <https://doi.org/10.1016/j.conbuildmat.2019.07.020>.
- [87] S. Wu, L. Pang, L. Mo, Y. Chen, G. Zhu, Influence of aging on the evolution of structure , morphology and rheology of base and SBS modified bitumen, *Constr. Build. Mater.* 23 (2009) 1005–1010. <https://doi.org/10.1016/j.conbuildmat.2008.05.004>.
- [88] W. Zhang, L. Zou, Z. Jia, F. Wang, Y. Li, P. Shi, Effect of Thermo-Oxidative Ageing on Nano-Morphology of Bitumen, 15 (2019). <https://doi.org/10.3390/app9153027>.
- [89] L.M. Rebelo, J.S. De Sousa, M. Pelissari, M. Aguiar, Aging of asphaltic binders investigated with atomic force microscopy, (2013). <https://doi.org/10.1016/j.fuel.2013.09.018>.
- [90] A. Koyun, J. Büchner, M.P. Wistuba, H. Grothe, Rheological , spectroscopic and microscopic assessment of asphalt binder ageing, (2020). <https://doi.org/10.1080/14680629.2020.1820891>.
- [91] M. Xu, J. Yi, Z. Pei, D. Feng, Y. Huang, Y. Yang, Generation and evolution mechanisms of pavement asphalt aging based on variations in surface structure and micromechanical characteristics with AFM, *Mater. Today Commun.* 12 (2017) 106–118. <https://doi.org/10.1016/j.mtcomm.2017.07.006>.
- [92] H.L. Zhang, H.C. Wang, J.Y. Yu, Effect of aging on morphology of organo-montmorillonite modified bitumen by atomic force microscopy, 242 (2011) 37–45. <https://doi.org/10.1111/j.1365-2818.2010.03435.x>.
- [93] A. Chen, G. Liu, Y. Zhao, J. Li, Y. Pan, J. Zhou, Research on the aging and rejuvenation mechanisms of asphalt using atomic force microscopy, *Constr. Build. Mater.* 167 (2018) 177–184. <https://doi.org/10.1016/j.conbuildmat.2018.02.008>.
- [94] L.D. Poulidakos, S. Santos, M. Bueno, S. Kuentzel, M. Hugener, M.N. Partl, Influence of short and long term aging on chemical , microstructural and macro-mechanical properties of recycled asphalt mixtures, *Constr. Build. Mater.* 51 (2014) 414–423. <https://doi.org/10.1016/j.conbuildmat.2013.11.004>.
- [95] Y. Yuan, X. Zhu, L. Chen, Relationship among cohesion , adhesion , and bond strength : From multi-scale investigation of asphalt-based composites subjected to laboratory-simulated aging, *Mater. Des.* 185 (2020) 108272. <https://doi.org/10.1016/j.matdes.2019.108272>.
- [96] H.L. Zhang, J.Y. Yu, Z.G. Feng, L.H. Xue, S.P. Wu, Effect of aging on the morphology of bitumen by atomic force, *J. Microsc.* 246 (2012) 11–19. <https://doi.org/10.1111/j.1365-2818.2011.03578.x>.
- [97] P.E.Y. Wang, K. Zhao, C. Glover, L. Chen, Y. Wen, D. Chong, Effects of aging on the properties of asphalt at the nanoscale, *Constr. Build. Mater.* 80 (2015) 244–254. <https://doi.org/10.1016/j.conbuildmat.2015.01.059>.
- [98] AASHTO standard practice R30. Standard practice for mixture conditioning of hot mix asphalt., n.d.
- [99] G.D. Danilatos, Mechanisms of detection and imaging in the ESEM, *J. Microsc.* 160 (1990) 9–19. <https://doi.org/10.1111/j.1365-2818.1990.tb03043.x>.



- [100] G.D. Danilatos, Introduction to the ESEM instrument, *Microsc. Res. Tech.* 25 (1993) 354–361. <https://doi.org/10.1002/jemt.1070250503>.
- [101] A.M. Donald, The use of environmental scanning electron microscopy for imaging wet and insulating materials, *Nat. Mater.* 2 (2003) 511–516. <https://doi.org/10.1038/nmat898>.
- [102] S.S.W. Tai, X.M. Tang, Manipulating biological samples for environmental scanning electron microscopy observation, *Scanning.* 23 (2001) 267–272. <https://doi.org/10.1002/sca.4950230407>.
- [103] M. Mazumder, R. Ahmed, A. Wajahat, S. Lee, SEM and ESEM techniques used for analysis of asphalt binder and mixture: A state of the art review, *Constr. Build. Mater.* 186 (2018) 313–329. <https://doi.org/10.1016/j.conbuildmat.2018.07.126>.
- [104] P. Mikhailenko, H. Kadhim, H. Baaj, Observation of bitumen microstructure oxidation and blending with ESEM Observation of bitumen microstructure oxidation and blending with ESEM, 0629 (2017). <https://doi.org/10.1080/14680629.2017.1304251>.
- [105] P. Mikhailenko, H. Kadhim, H. Baaj, S. Tighe, Observation of asphalt binder microstructure with ESEM, *J. Microsc.* 267 (2017) 347–355. <https://doi.org/10.1111/jmi.12574>.
- [106] K. Stangl, A. Jäger, R. Lackner, Microstructure-based identification of bitumen performance, *Road Mater. Pavement Des.* 7 (2006) 111–142. <https://doi.org/10.1080/14680629.2006.9690061>.
- [107] S.J. Rozeveld, E.E. Shin, A. Bhurke, L. France, L.T. Drzal, Network morphology of straight and polymer modified asphalt cements, *Microsc. Res. Tech.* 38 (1997) 529–543. [https://doi.org/10.1002/\(SICI\)1097-0029\(19970901\)38:5<529::AID-JEMT11>3.0.CO;2-O](https://doi.org/10.1002/(SICI)1097-0029(19970901)38:5<529::AID-JEMT11>3.0.CO;2-O).
- [108] J. Gaskin, On bitumen microstructure and the effects of crack healing, (2013).
- [109] P. Mikhailenko, C. Kou, H. Baaj, L. Poulidakos, A. Cannone-falchetto, J. Besamusca, B. Hofko, Comparison of ESEM and physical properties of virgin and laboratory aged asphalt binders, *Fuel.* 235 (2019) 627–638. <https://doi.org/10.1016/j.fuel.2018.08.052>.
- [110] L.D. Poulidakos, B. Hofko, A.C. Falchetto, L. Porot, G. Ferrotti, P. Mikhailenko, Recommendations of RILEM TC 252-CMB on the Effect of Short Term Aging Temperature on Long Term Properties of Asphalt Binder, Springer International Publishing, n.d. <https://doi.org/10.1007/978-3-030-00476-7>.
- [111] P. Mikhailenko, H. Baaj, C. Kou, J. Besamusca, B. Hofko, ESEM Microstructural and Physical Properties of Virgin and Laboratory Aged Bitumen, Springer International Publishing, n.d. <https://doi.org/10.1007/978-3-030-00476-7>.
- [112] E.E. Shin, A. Bhurke, E. Scott, S. Rozeveld, L.T. Drzal, Microstructure, Morphology, and Failure Modes of Polymer-Modified Asphalts, *Transp. Res. Rec.* 1535 (1996) 61–73. <https://doi.org/10.1177/0361198196153500109>.
- [113] H.H. Kim, M. Mithil, M.S. Lee, S.J. Lee, Identification of the microstructural components of crumb rubber modified asphalt binder (CRMA) and the feasibility of using environmental scanning electron microscopy (ESEM) coupled with energy dispersive X-Ray spectroscopy (EDX), *Int. J. Highw. Eng.* 18 (2016) 41–50. <https://doi.org/10.7855/IJHE.2016.18.6.041>.
- [114] B.V.R. Tata, B. Raj, Confocal laser scanning microscopy: Applications in material science and technology, *Bull. Mater. Sci.* 21 (1998) 263–278. <https://doi.org/10.1007/BF02744951>.
- [115] W.B. Amos, J.G. White, How the confocal laser scanning microscope entered biological research, *Biol. Cell.* 95 (2003) 335–342. [https://doi.org/10.1016/s0248-4900\(03\)00078-9](https://doi.org/10.1016/s0248-4900(03)00078-9).
- [116] M. Minsky, Memoir on inventing the confocal scanning microscope, *Scanning.* 10 (1988) 128–138. <https://doi.org/10.1002/sca.4950100403>.
- [117] N.S. Claxton, T.J. Fellers, M.W. Davidson, Laser scanning confocal microscopy, *Dep. Opt. Microsc. Digit. Imaging*, Florida State Univ. Tallahassee. (2006).
- [118] S.W. Paddock, Principles and practices of laser scanning confocal microscopy, *Mol. Biotechnol.* 16 (2000) 127–149. <https://doi.org/10.1385/MB:16:2:127>.
- [119] H. Li, W.K. Wan, Investigation of the asphaltene precipitation process from cold lake bitumen by confocal scanning laser microscopy, in: *SPE Int. Heavy Oil Symp.*, Society of Petroleum Engineers, 1995: pp. 709–740. <https://doi.org/10.2523/30321-ms>.
- [120] S. Bearsley, A. Forbes, R. G. Haverkamp, Direct observation of the asphaltene structure in paving-grade bitumen using confocal laser-scanning microscopy, *J. Microsc.* 215 (2004) 149–155. <https://doi.org/10.1111/j.0022-2720.2004.01373.x>.
- [121] J. Gong, Y. Liu, Q. Wang, Z. Xi, J. Cai, G. Ding, H. Xie, Performance evaluation of warm mix asphalt additive modified epoxy asphalt rubbers, *Constr. Build. Mater.* 204 (2019) 288–295.

- <https://doi.org/10.1016/j.conbuildmat.2019.01.197>.
- [122] R.J. Mikula, V.A. Munoz, Characterization of emulsions and suspensions in the petroleum industry using cryo-SEM and CLSM, *Colloids Surfaces A Physicochem. Eng. Asp.* 174 (2000) 23–36. [https://doi.org/10.1016/S0927-7757\(00\)00518-5](https://doi.org/10.1016/S0927-7757(00)00518-5).
- [123] E.M. A., S. Saman, M.L. N., H. Marwa, D.W. H., D. Samer, New Approach to Recycling Asphalt Shingles in Hot-Mix Asphalt, *J. Mater. Civ. Eng.* 24 (2012) 1403–1411. [https://doi.org/10.1061/\(ASCE\)MT.1943-5533.0000520](https://doi.org/10.1061/(ASCE)MT.1943-5533.0000520).
- [124] D. Grossegger, Microstructural aging of bitumen Microstructural aging of bitumen, in: 6th Eurasphalt Eurobitume Congr., 2016. <https://doi.org/10.14311/EE.2016.135>.
- [125] F. Handle, J. Füssl, S. Neudl, D. Grossegger, L. Eberhardsteiner, B. Hofko, M. Hospodka, R. Blab, H. Grothe, Understanding the microstructure of bitumen: a CLSM and fluorescence approach to model bitumen ageing behavior, in: Proc. to 12th ISAP Int. Conf. Asph. Pavements, Raleigh, USA, 2014.
- [126] F. Handle, H. Grothe, S. Neudl, Confocal laser scanning microscopy—observation of the microstructure of bitumen and asphalt concrete, in: 5th Eurasphalt Eurobitume Congr. Istanbul, 2012: pp. 13–15.
- [127] F. Handle, J. Füssl, S. Neudl, D. Grossegger, L. Eberhardsteiner, B. Hofko, M. Hospodka, R. Blab, H. Grothe, The bitumen microstructure: a fluorescent approach, *Mater. Struct.* 49 (2016) 167–180. <https://doi.org/10.1617/s11527-014-0484-3>.
- [128] Y.-J. Lee, L.M. France, M.C. Hawley, The Effect of Network Formation on the Rheological Properties of SBR Modified Asphalt Binders, *Rubber Chem. Technol.* 70 (1997) 256–263. <https://doi.org/10.5254/1.3538430>.
- [129] D. Kaya, A. Topal, T. McNally, Correlation of processing parameters and ageing with the phase morphology of styrene-butadiene-styrene block co-polymer modified bitumen, *Mater. Res. Express.* 6 (2019) 105309. <https://doi.org/10.1088/2053-1591/ab349c>.
- [130] H. Yin, Y. Zhang, Y. Sun, W. Xu, D. Yu, H. Xie, R. Cheng, Performance of hot mix epoxy asphalt binder and its concrete, *Mater. Struct.* 48 (2015) 3825–3835. <https://doi.org/10.1617/s11527-014-0442-0>.
- [131] Y. Liu, Z. Xi, J. Cai, H. Xie, Laboratory investigation of the properties of epoxy asphalt rubber (EAR), *Mater. Struct.* 50 (2017) 219. <https://doi.org/10.1617/s11527-017-1089-4>.
- [132] Y. Liu, J. Zhang, R. Chen, J. Cai, Z. Xi, H. Xie, Ethylene vinyl acetate copolymer modified epoxy asphalt binders: phase separation evolution and mechanical properties, *Constr. Build. Mater.* 137 (2017) 55–65. <https://doi.org/10.1016/j.conbuildmat.2017.01.081>.
- [133] Y. Jiang, Y. Liu, J. Gong, C. Li, Z. Xi, J. Cai, H. Xie, Microstructures, thermal and mechanical properties of epoxy asphalt binder modified by SBS containing various styrene-butadiene structures, *Mater. Struct.* 51 (2018) 86. <https://doi.org/10.1617/s11527-018-1217-9>.
- [134] Y. Liu, J. Zhang, Y. Jiang, C. Li, Z. Xi, J. Cai, H. Xie, Investigation of secondary phase separation and mechanical properties of epoxy SBS-modified asphalts, *Constr. Build. Mater.* 165 (2018) 163–172. <https://doi.org/10.1016/j.conbuildmat.2018.01.032>.
- [135] D. Großegger, Investigation of aged, non-aged bitumen and their bitumen fractions, (2015).